24 KSME Journal, Vol. 1, No. 1, pp.24~30, 1987.

MEASUREMENT OF TURBULENT DIFFUSION FIELD BEHIND A LINE HEAT SOURCE IN A HOMOGENEOUS SHEAR FLOW

Nam Ho Kyong* and Myung Kyoon Chung**

(Received January 8, 1987)

Turbulent diffusion behind a line heat source immersed in a nearly homogeneous shear flow is investigated. Test section of the wind tunnel is divided into 15 equal width channels equipped with adjustable internal flow resistances for the production of homogeneous shear flow. A combination of X-type hot wire for the measurement of velocity fluctuations and a cold wire for the measurement of temperature fluctuations has been devised to simultaneously obtain the cross correlations between the velocity and temperature fluctuations. The results show that all the distributions of velocity and scalar field are shifted toward the low velocity region of the homogeneous shear flow. The integral scales for velocity and scalar are different from each other in the shape of profiles so that the time scale ratio R does not remain constant. And the distributions of mean and fluctuating temperatures collapsed into a Gaussian curve by normalizing with mean half width and peak temperature.

Key Words : Uniform Shear Flow, Temperature Fluctuation, Cold Wire, Half Width, Turbulent Heat Flux, Integral Scale

NOMENCLATURE

d : Diameter of line heat source
e : Instantaneous voltage output from the linearized hot wire anemometer
E : Mean voltage output from the hot wire bridge
Eo : Mean voltage output from the hot wire bridge when the velocity is zero
G : Amplifier gain in cold wire circuit
H : Height of wind tunnel test section
L : Length scale
R : Time scale ratio
Re : Reynolds number based on the wire diameter
Ro : Reference electric resistance of platinum wire
T : Mean temperature
u,v : Fluctuating velocity components in axial and vertical directions, respectively
U,V : Averaged mean velocity component in axial and vertical directions, respectively
X : Axial distance from the exit of shear generator
x : Axial distance from the line heat source
y : Vertical distance from the line heat source
α : Sensitivity of linearlized hot wire anemometer to velocity
β : Sensitivity of linearized hot wire anemometer to temperature
II : Anisotropy
η : Temperature coefficient of platinum wire
Ψ : Effective Inclinations of the hot wire to the free-stream direction
θ : Fluctuating Temperature component
$\mathcal{I}_u$: Dynamic integral time scale
$\mathcal{I}_\theta$: Thermal integral time scale
ε : The dissipation rate of kinetic energy
ε_θ : The dissipation rate of thermal fluctuation

Subscripts

c : Center
eff : Effective
m(ax) : Maximum
p : At peak
1/2 : At half width

Superscripts

: Rms value
(—) : Conventional time average
* : Nondimensionalized quantity

*Korea Institute of Energy and Resources, Taejon 300, Korea
**Department of Mechanical Engineering, Korea Advanced Institute of Science and Technology, Seoul 131, Korea

1. INTRODUCTION

Many situations in nature and enginneering practice are closely related to the turbulent scalar diffusion; for instance, environmental meteorology, pollutant dispersions in atmospheric boundar layes, thermal pollutions and mixing of chemical species in a reaction, etc. Because of the significance of the turbulent scalar transport in a wide variety of engineering and natural systems, it has long been a desire to understand and to predict the turbulent scalar diffusion. A number of theoretical and experimental investigations have been brought out since the first theoretical formulations by G.I.Taylor(1921). However, there are still controversies about the mechanism of the turbulent diffusion even in the simplest type of turbulent flow, i.e., the grid-generated turbulence(Warhaft & Lumley 1978). For the dispersion in a grid-generated turbulence in a wind tunnel, Townsend(1951, 1954) measured the mean concentration profiles behind a point and a line heat source using the heat as a scalar contaminant, where it was concluded that the profiles are exactly Gaussian. Recently, the same experiment was repeated in more detail(Shlien & Corrsin, 1974) and the dispersion of particulate in the grid-generated turbulence was investigated by a light scattering technique(Gad-el-Hak & Morton, 1979). Turbulent dispersion in boundary layer was investigated more extensively because of its practical importance in the atmospheric dispersion of pollutants(Poreh & Cermak, 1964; Poreh & Hsu, 1971; Morkovin, 1966; Shlien & Corrsin, 1976). The higher order velocity-scalar correlations have been obtained recently(Raupach & Legg, 1983; Dekeyser & Launder, 1983) after the development of cold wire technique(LaRue et al., 1975) to measure the high frequency temperature fluctuations and the digital data processing technique.

But since the ordinary shear flows have complicated mean the shear patterns due to the rigid walls and turbulent/non

-turbulent interfaces, it is difficult to understand the role of mean shear on the turbulent scalar transport processes by the experimental data extracted from the turbulent dispersion in ordinary shear flows. Henceforth, it would be desirable to investigate the characteristics of turbulent scalar transport in a simplest shear flow, such as the uniform shear flow as a preceding step to understand the scalar transport processes in ordinary shear flows. In the present study, turbulent scalar field behind a line heat source immersed in a well-developed uniform shear flow is investigated experimentally in order to accumulate fundamental data to understand the scalar transport processes in turbulent flows. Simultaneous measurements of velocity and temperature fluctuation have been performed with a hot-and cold-wire combination to obtain mean fields and all second order correlations including turbulent heat fluxes and integral time scales.

2. EXPERIMENTAL APPARATUS AND INSTUMENTATION

An open return wind tunnel with test section of 0.6m x 0.6m x 12m(Fig.1) was specially designed for this study according to the design rules of Mehta and Bradshaw(1979). A multiblade fan with accelerating blade passage was driven by a variable speed motor of 11 kW, 4 pole with magnetic coupling. 9 : 1 contraction was used to get uniform flow in test section. The nonuniformity and turbulence intensity at the exit of contraction were within 1% and 0.3% respectively. The shear generator, located between exit of the contraction and the entrance of test section, is a revised type of that of Champagne, Harris and Corrsin(1970). The shear generator consists of 15 channels dividing the test section in equal height where the dampers for adjustment of internal flow resistance and horizontal bars are installed in each channel. In order to offer variable internal resistance in each channel, specially designed dampers are installed ; two identical rectangular-shaped plates with perforated rectangular holes are folded at the entrance of each channel, one of which is fixed and the other can slide over the other laterally.

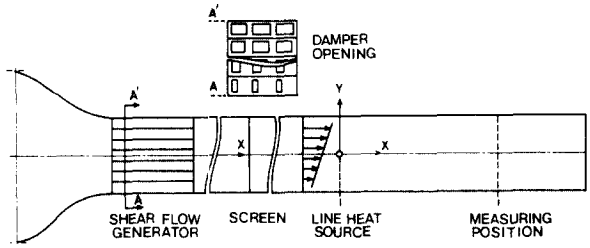

Fig. 1 Sketch of the homogeneous shear generator and a line heat source in a low speed wind tunnel.

As a line heat source, nichrome wire of 0.8mm diameter are stretched laterally at x/H=8, y/h=0.38 preventing the sagging of wire by suspending a weight of about 1kg.

Mean velocities in the test section were measureed by the standard Pitot tube with a micromanometer(Dwyer inc.) and hot wire anemometry is used to measure the velocity fluctuations. X-type hot wire probe (tsi model 1241) with a platinum wire of 6 μm diameter, 1.25mm length is powered by a constant temperature anemometer (tsi model 1050) to measure the axial & transverse velocity fluctuations. Polynomical linerarizers (tsi model 1052) and signal conditioner which is an active filter of attenuation rate 12 dB/octave (tsi model 1057) are followed to produce clean linearized outputs. Since the hot wire sensor responds to both the velocity and temperature fluctuations, velocity signals should be separated from the temperature signals. One of the methods to separate the signals can be found in Subramanian(1981) where the concept of the temperature sensitivity of the hot wire is used. Hot wires for present study are calibrated according to the following equations of linearized instantaneous output voltage :

$$e_1=\alpha_1(u+v\cot\Psi_1)+\beta_1\theta$$
$$e_2=\alpha_2(u+v\cot\Psi_2)+\beta_2\theta$$

$$\alpha_1=\frac{\partial E_1}{\partial U},\quad \alpha_2=\frac{\partial E_2}{\partial U},\quad \beta_1=\frac{\partial E_1}{\partial T},\quad \beta_2=\frac{\partial E_2}{\partial T}$$

where α's, β's and Ψ's are determined by a cold jet calibration, hot jet calibration and yaw test, respectively.

For the measurement of temperature fluctuations, a cold wire (or resistance termometer) was chosen because of its outstanding accuracy and high frequency response makes it botter than any other sensors.

A home-made electronic circuit with dry batteries was used to operate the cold wire of 0.63 μm diameter platinum wire. -3 dB point in the frequency response is estimated to be about 6 kHz according to the works of LaRue, Deaton and Gibson(1975). Instantaneous temperature can be obtained by the following equation ;

$$E=G\cdot I\cdot R_o\cdot\eta\cdot T$$

From the experiment on hot jet, the temperature coefficient was obtained be $\eta=0.0035\pm0.0001$ 1/℃. A schematic diagram of instrumentation for the simultaneous measurement is shown in Fig. 2.

Simultaneous digitizations of the analog signals from 3-channels were carried out with analog to digital converter(A/D converter) attached in the data processing unit(Data 6000, Data Precision Co.). The A/D converter can digitize 4 channels simultaneously with 25 kHz sampling rate for each channel since the maximum sampling rate is 100 kHz. The resolution was 14 bit, by which 0.6 millivolt can be distinguished. Since the frequency response of the tape recorder is 5 kHz (15kHz for hot wire, 6 kHz for cold wire), Nyquist cutoff frequency for digitizations is 10 kHz. Slower sampling rate is permissible for the calculations of moments, but cannot be permitted for those of autocorrelation because the reciprocal of the sampling rate becomes the interval between the data for the autocorrelation in the digital data processing technique. If this interval is not sufficiently small compared to the integral time scale, the shape of autocorrelation obtained from the digital data processing has an aliasing problem.(Bendat & Piersol, 1971).

The diskette driver of D-6000 is composed of dual channel, designed for 5 1/4″ floppy diskette, where 2.8×10^4 data can be stored at a time. D-6000 has "built in" digital circuits for the calculations of all moments, auto- or cross-correlations, spectra, probability density function, etc. D-6000 is intefaced with the PET4032 for remote control of the data acquisition as well as for computing various turbulent quantities. At each measurement position, 10 records of 2048 samples per channel have been stored in floppy diskettes which correspond to two second data stored in floppy diskettes which correspond to two second data duration. Since the dynamic integral time scale is about 5 milliseconds, the data duration is 400 times the integral time scale which is thought to be long enough for the calculation of higher order moments or velocity-scalar cross correlation(Fabris, 1983).

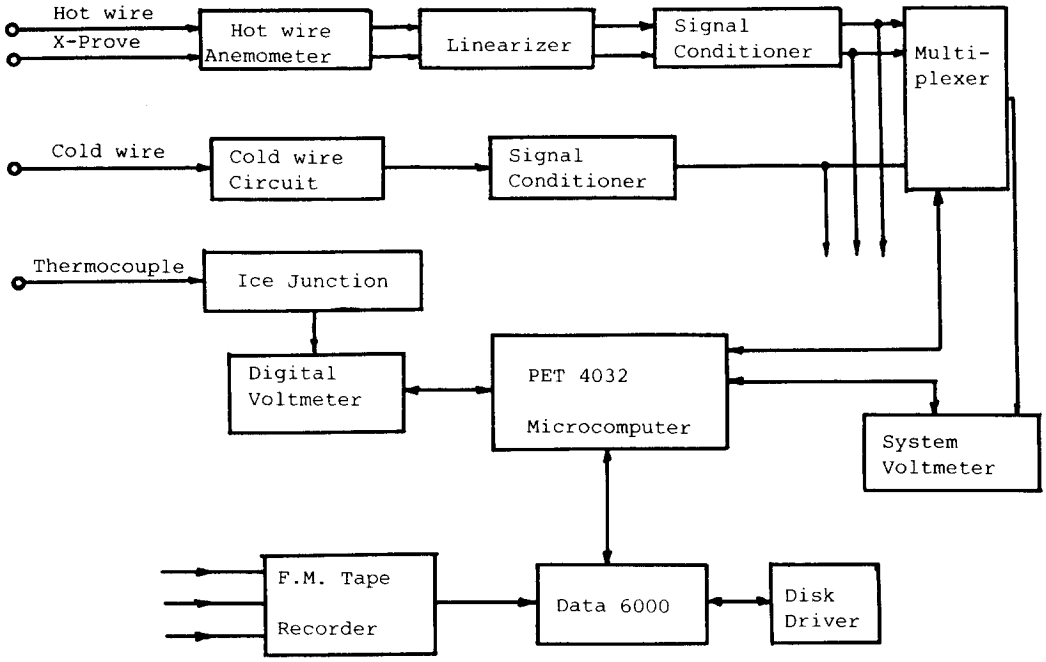

Fig. 2 Instrumentations for the measurement of velocity and temperature fluctuations.

3. RESULTS AND DISCUSSIONS

3.1 Effective Strength of the Line Source and Scaling of Data

The heat released from the line heat source is partly lost to surroundings by radiation of the wire and by heat conduction through the duralumin junctions. The wire temperature was about 340℃. The radiation heat loss was estimated to be about 8W and the conduction heat loss about 15W. In addition, there may be a convection heat loss through the walls(Raupach & Legg, 1983). However, since the temperature difference between the wire and the side wall was less than 2℃, such heat loss should be negligible. As a result, the effective heating rate was estimated to be about 160W.

The time scale of the large eddy motion is imposed by the mean strain rate S of 3.38 sec^{-1}; therefore, the relevant time scale T should be 0.296 seconds. A convective length scale is determined by the relation $Lx = UcT$ where Uc is the centerline mean velocity of 7.85m/sec, hence, $Lx = 2.32m$. Usually a diffusive length scale L of thermal wake or jet is taken to be either the half-width $L_{\frac{1}{2}}$ of the mean temperature profile or $Ly = v\mathcal{J}$ where v is the r.m.s. vertical velocity fluctuation and $\mathcal{J}$, the integral time scale(Tennekes & Lumley, 1972 ; Dupont et al. 1985). The latter is considered to be physically more appropriate, though the half-width $L_{\frac{1}{2}}$ is used to non-dimensionalize the data presented in this paper for clarity.

Finally a temperature scale θ_s must be chosen such that the maximum temperature excess Tmax scaled by θ_s should be of order unity. In this study θ_s is defined by a relation(Raupach & Legg, 1983), $\theta_s = q/(\rho CpUcL_{\frac{1}{2}})$ where q is the heating rate per unit length of wire, ρ the density of air and Cp is the specific heat of air at constant temperature. Since the maximum temperature excess Tmax is a more clearly measurable value compared with the deduced quantity θ_s with less certainty, the data in the next section will be non-dimensionalized by Tmax.

3.2 The Mean Fields of Velocity and Temperature

Mean velocities measured using the standard Pitot tube with and without the heating wire are shown in Fig.3. The solid line represents the mean velocity profiles in the wind tunnel without the line heat source. The distribution without the heating wire show very good linearity. The portion of the uniform shear in the measuring section are about 70% of the test section height. The upper boundary layer was about 20% and 10% for lower boundary layer The rapid growth of the upper boundary layer thickness is attributed to the mometum transport toward the lower velocity region due to the mean shear. The velocity distributions at the position 100mm apart from the centerline were measured to test the

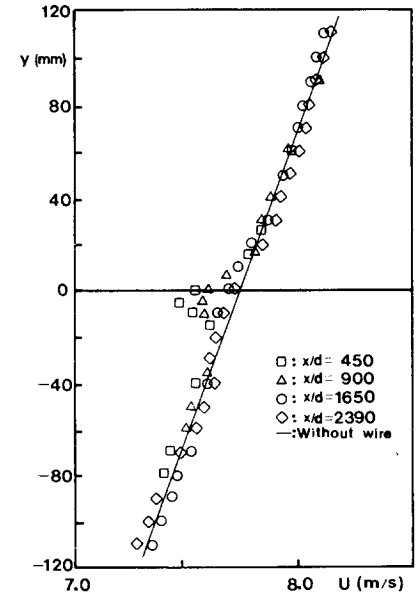

Fig. 3 Mean velocity distributions in the range of measurement with and without the heating wire.

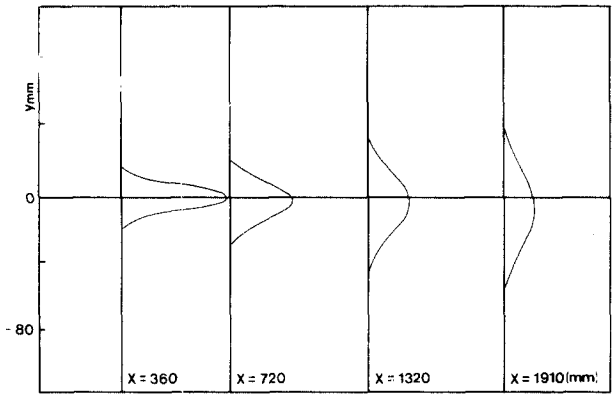

Fig. 4 Evolution of the mean tenperature distribution along the downstream distance.

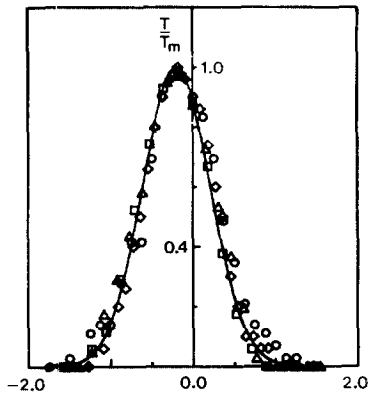

Fig. 5 Normalized mean temperature distributions. Symbols as in Fig. 3.

transverse homogeneity, but they also fit to the single line in Fig.3. Since the wire diameter is not small enough, there is an appreciable wake pattern behind the line heat source as shown in Fig. 3. As can be shown in Fig. 3., the wake pattern nearly disappears after x=1910mm from the source. It was found that the mean velocity wake virtually disappears at a downstream distance equivalent to a convective length scale Lx from the source.

The mean temperature field was measured by the thermocouple for the two heating rates. The evolution of the mean temperature field is shown in Fig 4. and the same data are normalized by appropriate length scales and are shown collectively in Fig. 5.

Table 1 Downstream variations of T_{max}, θ_s, $L_{\frac{1}{2}}$ and δ

Distance x/L_x	0.155	0.31	0.569	0.823
Maximum temperature T_{max}, ℃	1.72	1.03	0.72	0.50
Temperature scale θ_s, ℃	1.65	1.04	0.68	0.51
Temperature half-width $L_{\frac{1}{2}}$,mm	17.0	26.5	41.0	54.2
Downward shift of peak temperature δ, mm	−4.5	−6.0	−7.7	−10.0

As can be seen in the figure, the mean temperature profiles follow approximately the Gaussian distribution with gradual downward shift of the centerline along the downstrem distance. Small asymmetry of the temperature profiles attributes to the effect of the velocity wake and the mean shear. The asymmetry is smaller than that in Tavoularis & Corrsin(1980) who used much stronger shear rate of 46.8 sec^{-1}. In

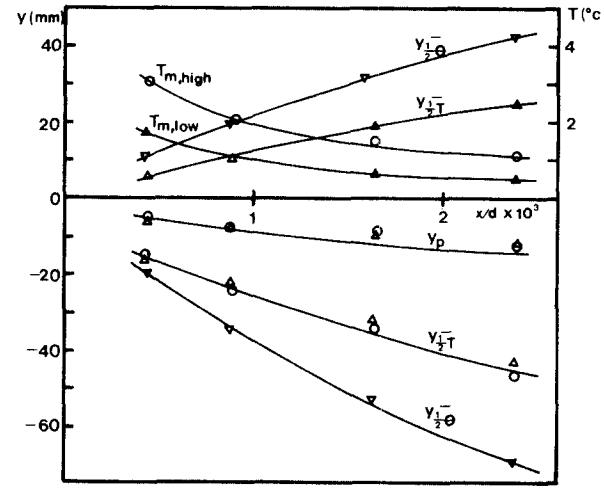

Fig. 6 Axial development of peak temperatures and half widths.

the upper part, the effective shear is stronger than that in the lower part and thus the turbulent kinetic energy is generated more in the upper part than in the lower part. This causes a greater spread of scalar quantities in the upper part of the heated wake than in the lower part, which is consistent with Hinze(1975). It is interesting to note that the non-dimemsionalization of the y distance with the temperature half width $L_{\frac{1}{2}}$ allows the center position of each profile to coincide each other. The maximum mean temperature excess T_{max}, downward shift of the center of the Gaussian profile δ, the temperature half width $L_{\frac{1}{2}}$ and the temperature scale θ_s are tabulated in Table 1., and the downward developments of the temperature half width $y_{\frac{1}{2}T}$, half width of rms temperature $y_{\frac{1}{2}\theta}$ and T_{max} are shown in Fig.6.

It is found that θ_s is indeed of the similar magnitude to T_{max} and thus the product of T_{max} and $L_{\frac{1}{2}}$ remains at similar value as was pointed out by Warhaft(1984).

3.3 Integral Time Scales and Dissipations

The integral time scale variation of velocity and temperature are depicted in Fig. 7a and b. The time scale was obtained by integrating the auto-correlation curve up to the zero crossing point(Champagne at al., 1970).

Due to the velocity wake, the velocity timescale varies

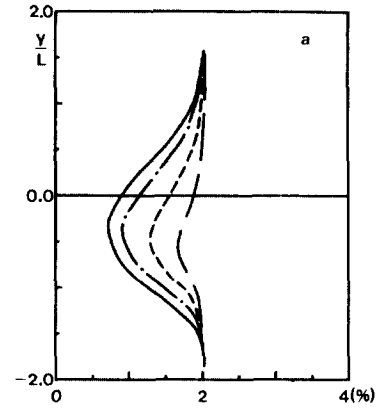

Fig. 7a Normalized time scales for velocity, $\mathcal{T}/T$: ——, X/Lx=0.155 ; — · —, X/Lx=0.32 ; ·····, X/Lx=0.569 ; - -, X/Lx=0.823.

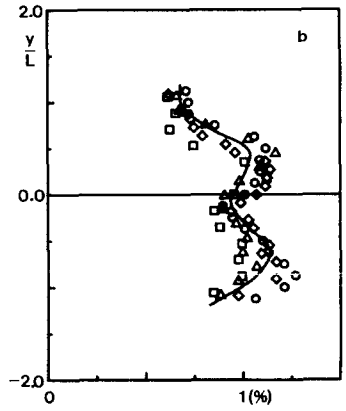

Fig. 7b Normalized time scales for temperature, $\mathcal{J}_\theta/T$; Symbols as in Fig. 3.

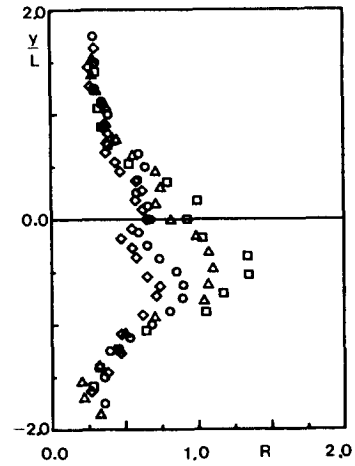

Fig. 8 Time Scale ratio, $R=(\mathcal{J}_\theta/\mathcal{J})$ symbols as in Fig. 3

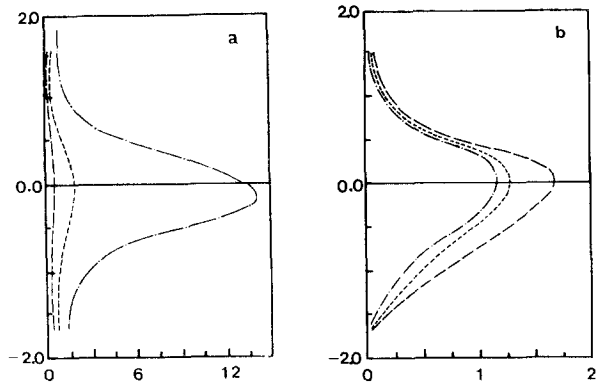

Fig. 9a Dissipation profiles ; $\varepsilon^*=\varepsilon/(L^2T^{-1})$, where T is the imposed time scale, T=0.296 sec ; Curves as in Fig. 7a

Fig. 9b Dissipation profiles ; $\varepsilon_\theta^*=\varepsilon_\theta/(T_{max}^2\,T^{-1})$, where T is the imposed time scale.

significantly in the range of experiment, whereas the temperature timescale remains more of less the same along the downstream distance. The location of the peak $\mathcal{J}_\theta$ coincides with the position of maximum slope of the θ' profile (see Fig. 11). The integral timescale ratio $R(=\mathcal{J}_\theta/\mathcal{J}_\mu)$ at the edge of the wake profile is about 0.3 and within the wake region it varies between 0.5 and 1.3(Fig.8). Higher value in the lower part attributes to the down shift of larger thermal mass. The rate of kinetic energy dissipation ε and the destruction of temperature variance ε_θ which are non-dimensionalized by local scales are obtained as in Figs. 9a to b. It is seen that ε decreases much faster than ε_θ along the downstream distance.

3.4 The Second Order Moments ; $\overline{u_iu_j}$, $\overline{\theta^2}$ and $\overline{u_j\theta}$

The r.m.s. values of the axial and vertical velocity fluctuations u' and v' are non-dimensionalized by the center line mean velocity U_c at the source and are shown in Fig.10. Compared with the wake structure in the mean velocity profile, the wake of the turbulent fluctuations persists comparatively longer due to the production of the turbulent kinetic energy by an amount $-\overline{uv}\,dU/dy$. This is consistent with other observations(Shlien & Corrsin, 1976 ; Champagne et al, 1970) In comparison with this persistence of the wake property with the measurement of Raupach & Legg(1983) in a turbulent boundary layer, the restoration to the free stream condition is rather slower in the present experiment. This is due to the lower turbulent intensity of the present study rather than that in the turbulent boundary layer flow. In the usual two-dimensional wake behind a cylinder, u'-distribution has two peaks at both sides of the wake even in the self-preservation region(Townsend, 1976). But in our case, since the two peaks of u' profile formed in the initial stage of evolution,are exposed to two differently straining field, i.e., high shear in the upper part and low shear in the lower part, the bulge of the u' value in the upper part and the shrinkage in the lower part together make the u' profile to merge into the u'-profile of a single peak. The v'-distribution in Fig.10b has similar structure to that of u'-distribution. The profile skews in the lower side and the peak position tends to shift upward. Both the u' and v' values at the centerline approach to the free stream values far downstream. Distribution of the mean Reynolds shear stress $\overline{uv}$ displayed in Fig. 10c is similar in shape to the plane wakes and jets(Fabris, 1979). It appears that the profile is a superposition of the plane wake to the homogeneous uniform shear flow with smaller spread rate of the profile in the upper part than that in the lower part. It was not clear how to identify the measure of downward shift of the dynamic field. The point of maximum mean velocity defect almost coincides with the point of zero crossing of the $\overline{uv}$ profile, while the point where the $\overline{uv}$ profile in the wake zone has the free stream value is approximately the same as the mid-point of the mean velocity profile. At far downstream, $\overline{uv}$ profile does not cross the zero level. It is also noted that the points of free stream value of $\overline{uv}$ collapse on a single point when y distance is scaled by $L_{\frac{1}{2}}$. Therefore, the point at which the $\overline{uv}$ has the same value as the free stream is considered to be appropriate measure of the downward deflection of the dynamic(or velocity) field. The r.m.s. temperature fluctuations are shown in Fig.11. where θ' is normalized by the maximum temperature excess T_{max}.

Compared with the spread of the mean temperature profile, the spread of θ' is wider by about 20%. The θ'-distribution has double-peaks at all x positions. The appearance of the double peaks was explained by Warhaft(1984) and also theoretically predicted by Stapountzis et al(1986). Although both these previous studies show that the double-peak disappears at x/M=1.8 where M is the mesh size of the grid (which is approximately equivalent to our diffusive length scale Lv), such double-peak persists far downstream in the present cause as in Tavoularis & Corrsin(1980). Warhaft(1984) reported re-emergence of the double-peak after a

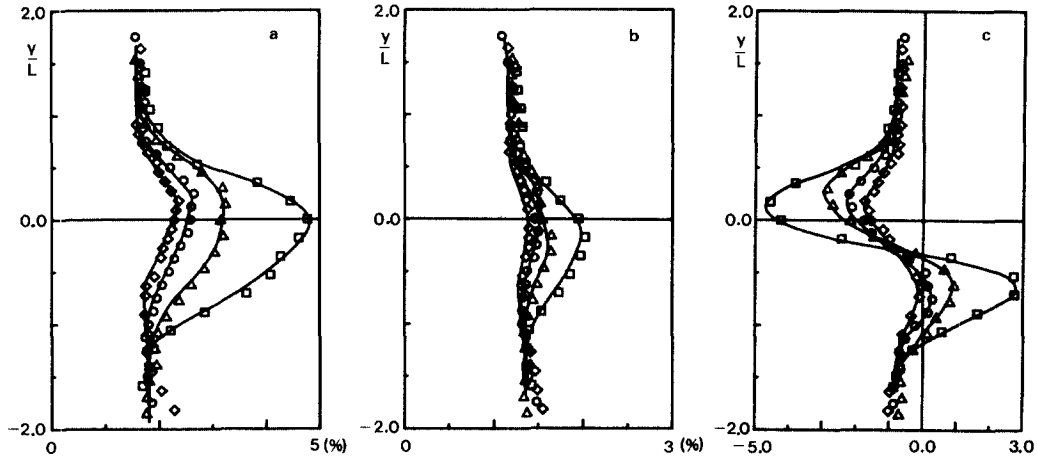

Fig. 10 Distributions of Reynolds stress : (a) u'/U_c, (b) v'/U_c, (c) $\overline{uv}/U_c^2 \times 10^4$

long distance downstream, but, such phenomena could not be observed. The ratio of θ'_{max} to the maximum mean temperature excess T_{max} was reported to be about 0.7 in Warhaft and 0.6 in Stapountzis et al., but in our case the ratio is about 0.4. Considering the value of 0.27 obtained by Fabris(1979) who used a thick cylinder of diameter 6.2mm, such difference in the ratio is due the the source wire size ; the ratio becomes larger for smaller wire size. The θ'-distribution has a slight asymmetry with wider spread in the lower part. Fig.12 shows profiles of the vertical heat flux $\overline{v\theta}$. The downward deflection at each measurement position is indicated by the zero crossing point which is almost conincident with the T_{max}. The $\overline{v\theta}$ profile shape is of anti-symmetricity with a little smaller peak value in the lower part. This implies that the vertical heat flux upward is larger than that in the downward direction. The weakness of the mean shear effect on $\overline{v\theta}$ is due to the fact that production term in $\overline{v\theta}$ equation does not contain the mean shear or the Reynolds shear stress $\overline{uv}$. The overall shape of $\overline{v\theta}$ is very much similar to that in a plane heated wake(Fabris, 1979) ; the mean shear only indirectly has small effect on the $\overline{v\theta}$ profile. Contrarily to the $\overline{v\theta}$ profile, the streamwise heat flux $\overline{u\theta}$ shown in Fig. 12 has a strong effect of the mean shear. One of the production terms in the governing equation for $\overline{u\theta}$ is $-\overline{v\theta}\, dU/dy$ whose magnitude is of significant size throughout the field of measurement. The higher value in the upper part is due to the larger value of $\overline{v\theta}$ and faster local mean velocity there. Note that $\overline{u\theta}$ has negative sign in the whole field as in the plane heated wake. However, in a dispersion measurement in a turbulent boundary layer, $\overline{u\theta}$ gradually changes sign from negative to positive when the wall is approached. Fig. 13 shows the decay of anisotropy II and $II_c$and the variation of the time scale ratio R along the centerline. The anisotropy II is defined by $II = b_{ij}\, b_{ij}$ where $b_{ij} = \overline{u_i u_j}/q^2 - 1/3\delta_{ij}$. The scalar anisotropy II_c is defined by $II_c = f_i f_j$where $f_i = \overline{u_i\theta}/q\theta'$, $q^2 = \overline{u_i u_j}$.

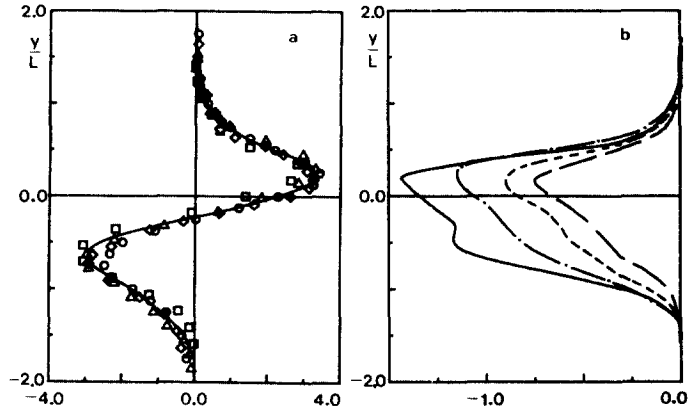

Fig. 12 Turbulent heat flux distributions ; (a) the vertical heat flux $\overline{v\theta}/U_c T_{max} \times 10^3$, (b) the streamswise heat flux $\overline{u\theta}/U_c T_{max} \times 10^2$, Symbols as in Fig. 3 and curves as in Fig. 7a.

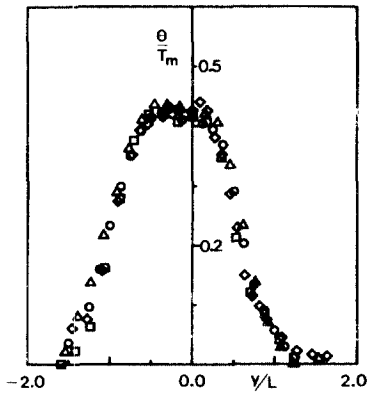

Fig. 11 The r.m.s. temperature fluctuations ; Symbols as in Fig. 3.

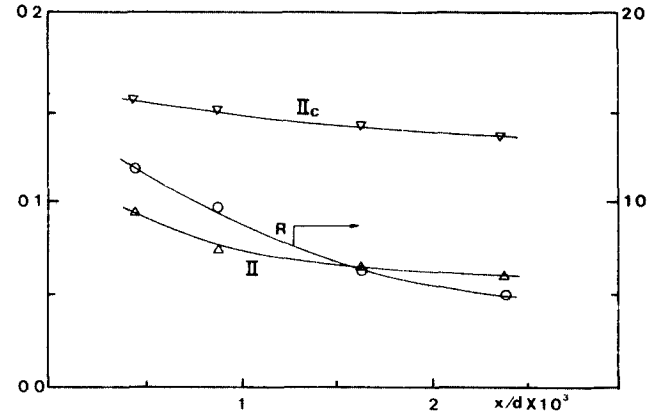

Fig. 13 Anisotropy and time scale ratio along the centerline.

It is shown that the anisotropies II and II_c both relax to isotropic state at almost the same rate. The time scale ratio R approaches to about 0.5 at far downstream.

4. CONCLUSIONS

This paper has presented an experimental investigation on the turbulent dispersion of passive temperature behind a line heat source in a homogeneous uniform shear flow. The results can be summarized as follows:

(1) It was found that the vertical profiles of the mean temperature and r.m.s. temperature both exhibit Gaussian distributions except a little degradation in the center region of the r.m.s. temperature profiles.

(2) The mean temperature data at different downstream distances can be well collapsed onto a simple Gaussian curve with reasonable scatter when they are normalized by the local peak mean temperature and the local temperature half width.

(3) Profiles for statistical moments of velocity fluctuations and rate of dissipation change appreciably with the downstream distance due to the presence of the wake structure. However, the thermal statistics changes slowly with the downstream distance.

(4) The vertical heat flux $\overline{v\theta}$ normalized by local scales remain the same with the downstream distance, while the streamwise heat flux $\overline{u\theta}$ shows severe evolution.

(5) The time scale ratio is between 0.5 and 1.3 across the stream and it asymptotes to a value of 0.5 at far downstream.

It is believed that comparative study of this data with previous experiments on thermal turbulence in a grid-generated isotropic turbulence and a boundary layer turbulence should reveal conclusive information on the role of straining effect on the temperature field.

ACKNOWLEDGEMENTS

This research was supported by the Korea Science and Engineering Foundation under Grant No. 812-09-013-2.

REFERENCES

Bendat, J.S. and Piersol,A.G., 1971, "Random Data", Wiley and Sons

Champagne, F.H., Harris V.G. and Corrsin, S., 1970, "Experiments on Nearly Homogeneous Turbnulent Shear Flow", J. Fluid Mech., Vol, 41, pp.81~139.

Dekeyser, I. and Launder, B.E., 1983, "A Comparison of Triple Moment Temperature-Velocity Correlations in the Asymmetric Heated Jet with Alternative Closure", Turbulent Shear Flow 4, pp. 102~120, Springer-Verlag.

Dupont, A, Kabiri, M.EL and Paranthoen, P., 1985, "Dispersion From Elevated Line Source in a Turbulent Boundary Layer", Int. J. Heat Mass Transfer, Vol. 28, No. 4, pp.892~894.

Fabris, G., 1979,"Conditional Sampling Study of Turbulent Wake of a Cylinder", J. Fluid Mech., Vol. 94. pp.673~709.

Fabris, G., 1983, "Third Order Conditional Transport Correlations in the Two-dimensional Turbulent Wake", Phys. of Fluids, Vol. 26, No 2, pp.422~427.

Gad-el-Hak, M and Morton, J.B., 1979, "Experiments on the Diffusion of Smoke in isotropic Turbulent Flow, AIAA, Vol. 17, Vol. No 6,

Hinze, J.O., 1975, "Turbulence", 2nd ed., McGraw-Hill

LaRue, J.C., Deaton, T, and Gibson, C.H., 1975, "Measurement of High Frequency Turbulent Temperature", Rev. Sci. Instru., Vol.46, p.757.

Mehta, R.D. and Bradshaw, P., 1979, "Design Rules for Small Low Speed Wind Tunnels", Aeronautical Journal, Vol. 5, p.443.

Morkovin, M.V., 1965, "On Eddy Diffusivity, Quasi-Similarity and Diffusion Experiments in Turbulent Boundary Layer", Int, J. Heat Mass Transfer, Vol. 8, pp.129~145.

Poreh, M. and Cermak, J.E., 1964, "Study on Diffusion From a Line Source in a Turbulent Shear Flow", Int.J. Heat Mass Tranf., Vol. 7, pp.1083~1095.

Poreh,M. and Hsu,K.S., 1971, "Diffusion From a Line Source in a Turbulent Boundary Layer", Int. J Heat Mass Transf. Vol. 14, pp.1473~1483.

Raupach, M.R. and Legg, B.J., 1983, "Turbulent Dispersion From Elevated Line Source", J. Fluid Mech., Vol. 136, pp.111~137.

Shlien, D.J. and .Corrsin, S., 1974, "A measurement of Lagrangian Velocity Autocorrelation in Approximately Isotropic Turbulence", J. Fluid Mech., Vol. 62, No. 2.

Shlien, D.J. and Corrsin, S., 1976, "Dispersion Measurement in a Turbulent Boundary Layer", Int. J. Heat Mass Transfer, Vol. 19, pp.285~295.

Stapourtzis, H., Sawford, B.L., Hung, J.C.R. and Britter, R. E., 1986, "Structure of the Temperature Field Downwind of a Line Source in Grid Turbulence", J. Fluid Mech., Vol. 165, p.401.

Subramanian, C.S., 1981, "Some Properties of the Large Scale Structure in Slighly Heated Turbulent Boundary Layer", Ph.D. Thesis, University of Newcastle, Australia.

Tavoularis, S. and Corrsin, S., 1980, "Experiments in Nearly Homogeneous Turbulent Shear Flow with a Uniform Mean Temperature Gradient", J. Fluid Mech., Vol. 104, pp. 317~347.

Taylor, G.I., 1921, "Diffusion by Continuous Movement" Proc.London Math. Soc, Vol. 2, No. 20.

Tennekes, H. and Lumley, J.L., 1976, "A First Course in Turbulence", MIT Press.

Townsend, A.A., 1951, "The Diffusion of Heat Spots in Isotropic Turbulence", Proc. Roy. oc., A209, pp.418~430.

Townsend, A.A., 1954, "The Diffusion Behind a Line Source in Homogeneous Turbulence, Proc. Roy.Soc. A224, pp.487~512.

Townsend, A.A., 1976, "The Structure of Turbulent Shear Flow", 2nd ed., Cambridge Univ. Press.

Warhaft, Z. and Lumley, J.L., 1978, "An Experimental Study of the Decay of Temperature Fluctuations in Grid-Generated Turbulence", Vol. 88, pp.659~684.

Warhaft, Z., 1984, "The Interference of Thermal Fields From Line Sources in Grid Turbulence", J. Fluid Mech., Vol. 144, pp.363~387.